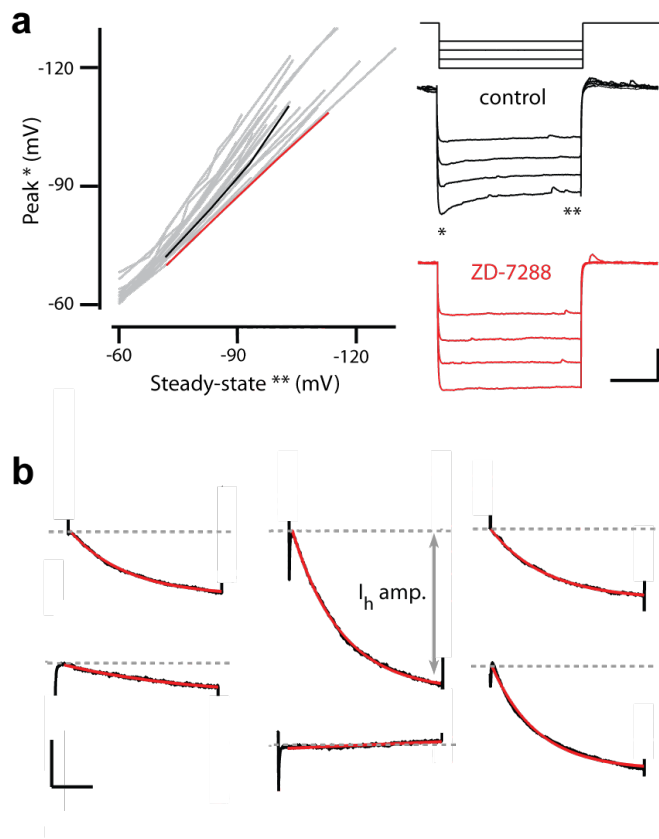
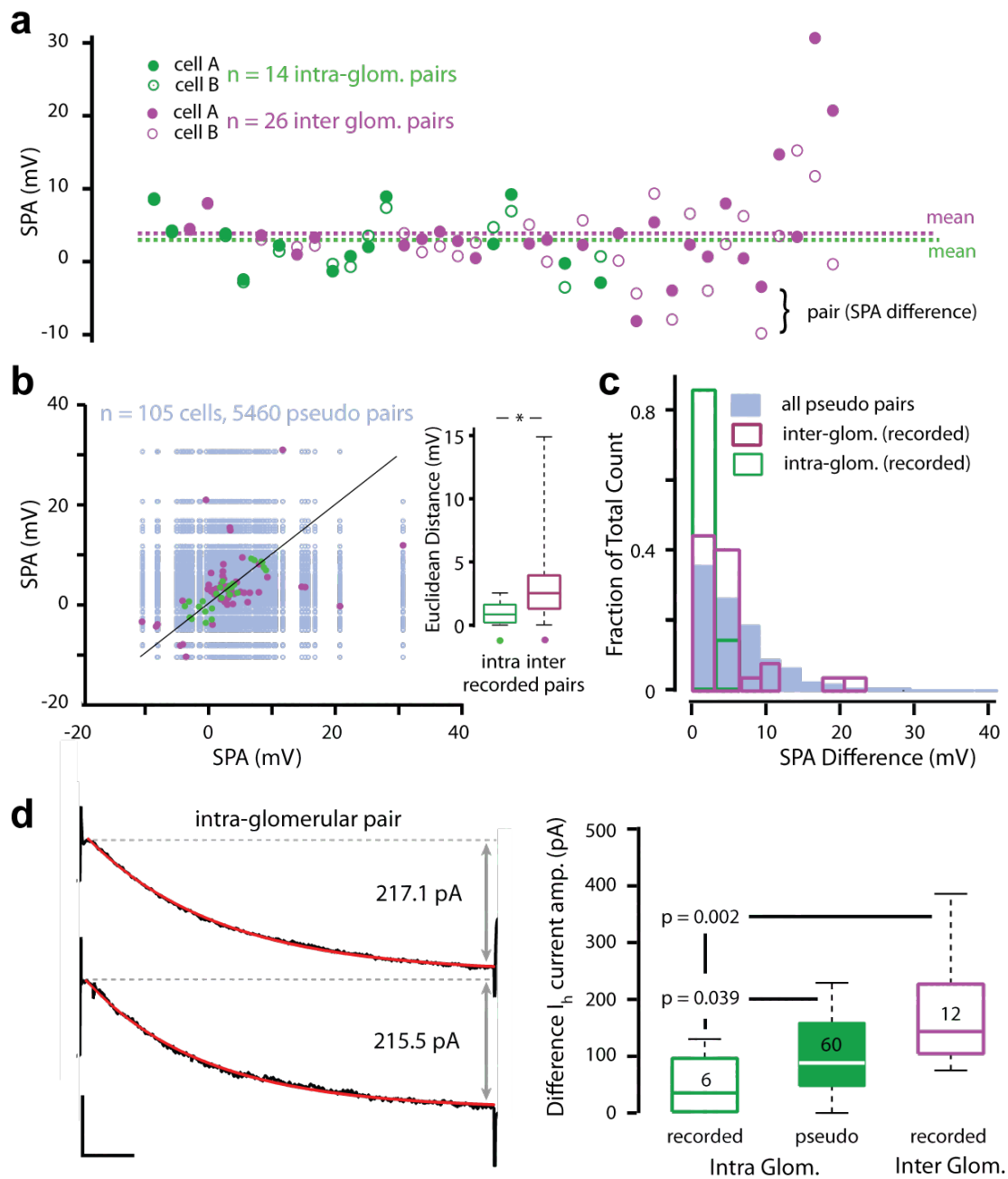


SUPPLEMENTARY FIGURES



Supplementary Figure 1:
Diversity of the hyperpolarization-evoked sag potential and I_h current recorded in mouse mitral cells
a) Plot of sag peak versus steady-state membrane potential for individual mitral cells recorded randomly across the olfactory bulb (n = 21 cells, n = 4 mice). Each grey line represents an individual cell. Black and red lines indicate the peak versus steady-state relation for one cell in the absence (black) and presence (red) of ZD-7288. Right: Example membrane voltage traces recorded during negative current step injections (step sizes of 100 pA) used to quantify the sag potential amplitude for the cell highlighted in the plot. Sag amplitude is calculated as the difference between the peak* and steady-state**.

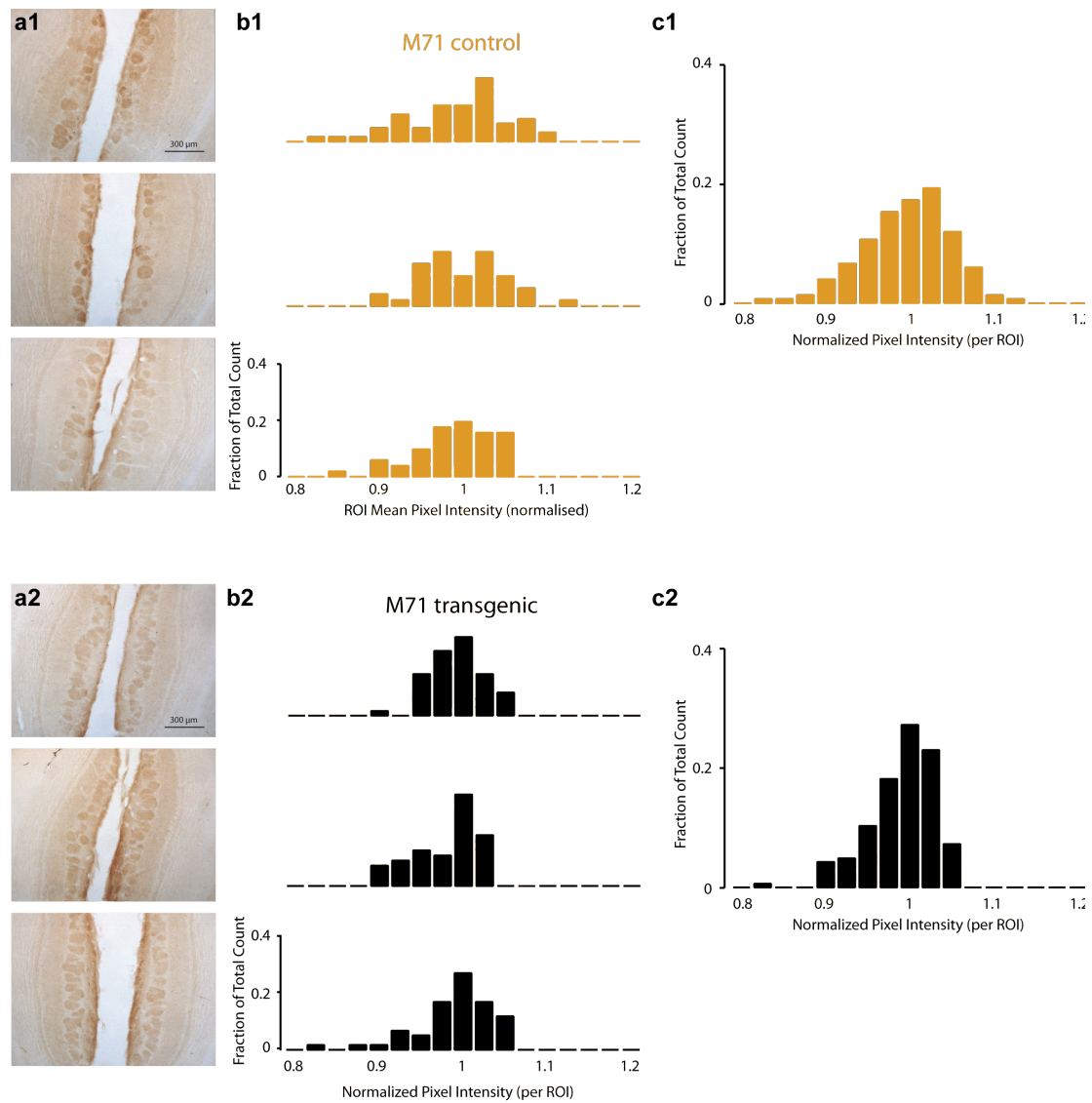
Scale bar is 1 sec and 20 mV. **b)** Averages of 5-10 digitally subtracted current traces (+/- ZD-7288, see methods) recorded from six different cells in voltage clamp mode in the presence of the I_h -isolation cocktail (current amplitude range 0 - 645 pA, mean = 174 pA, s.d. = 173 pA, median = 125 pA, n = 44 cells). Traces fitted with an exponential function to determine current amplitude (red traces, see methods). Scale bar = 0.5 sec, 200pA.



Supplementary Figure 2: Sag potential and I_h current amplitude differences recorded in intra-, inter- and pseudo-pairs in wild-type mice.

a) Plot showing the relation between SPA amplitude within individual cells and the difference between their simultaneously recorded partner (inter-glom. purple, intra-glom. green). Pairs are plotted according to their SPA difference (increasing from left to right). b) Scatterplot of pseudo pairs extrapolated from the SPA values obtained

from all recorded mitral cells (blue, $n = 105$). Overlaid are the recorded values determined for each inter- and intra- glomerular recorded pair. Recorded SPA values are plotted twice and are thus symmetrical about the unity line. Analysis was performed only on one data point per pair. The perpendicular distance from the unity line was calculated for each pair and is plotted in the inset containing the box plots ($p = 0.002$, MWU). **c)** Histogram of total counts of SPA differences obtained by multiple pair-wise comparison of all recorded mitral cells in wild-type animals ($n = 5460$ pseudo pairs generated from 105 recordings; bin size = 3 mV; blue). Overlaid is the histogram of SPA differences for simultaneously recorded inter-glomerular pairs (purple) highlighting the similarity of the two distributions. Also overlaid is the histogram of SPA differences for simultaneously recorded intra-glomerular pairs (green). **d)** Averages of 5-10 digitally subtracted current traces (\pm ZD-7288) obtained from a recorded intra-glomerular pair of mitral cells in the presence of the I_h isolation cocktail (see methods) overlaid with an exponential fit (red). Scale bar: 100pA and 250ms. Boxplot of voltage clamped recorded intra- pairs ($n = 6$, green open) and pseudo pairs ($n = 60$, green solid) and recorded inter-glomerular mitral cells ($n = 12$ pairs; purple). P values are reported for a one-way MWU test.



Supplementary Figure 3: Glomerular-based HCN2 expression in M71tg and control mice.

Images of HCN2-DAB stains from three different M71 control (**a1**) and transgenic (**a2**) mice. **b1**) Histograms of mean pixel intensity for glomerular regions of interest (ROIs) normalized to the median values for each M71 control (n = 144 ROIs) and transgenic (n = 158 ROIs, **b2**) mouse. All histograms are vertically aligned and on the same vertical and horizontal scale. Pooled data from all M71 control (**c1**, n = 3) and transgenic mice (**c2**, n = 3).

ONLINE METHODS

Current Clamp Recordings

Horizontal olfactory bulb slices (300 μ m) were prepared from wild-type C57Bl/6J (P21-P35) and M71 transgenic (129SvEv X C57Bl/6J) or M71 control littermates (M71 control) aged 4–6 weeks. All procedures were carried out in accordance with the UK Home Office and The Danish National Committee for Ethics in Animal Research. Whole-cell recordings were performed using a 700A or B Multiclamp amplifier and data were acquired with the Nclamp/Neuromatic package (J. Rothman, <http://www.thinkrandom.com/>) running under Igor Pro using an ITC-18 interface or a M-series DAQ device from National Instruments as previously described¹. Glass electrodes were pulled to a resistance of 5–9 M Ω and were filled with an internal solution containing (mM): 130 methanesulphonic acid, 10 Hepes, 7 KCl, 0.05 EGTA, 2 Na₂ATP, 2 MgATP, 0.5 Na₂GTP and 0.4% biocytin, KOH titrated to pH 7.2. The recordings were performed at 35–37°C. The external recording and slicing solution contained (in mM): 125 NaCl, 2.5 KCl, 2 CaCl₂, 1 MgCl₂, 25 NaHCO₃, 1.25 NaH₂PO₄ and 25 D-glucose, perfused with 95% O₂ and 5% CO₂. Only cells with somata residing in the mitral cell layer were recorded in this study.

Paired Recordings and Electrical Coupling

We used electrical coupling to unambiguously determine whether or not the tufts of two mitral cells share the same glomerulus¹⁻³. By alternating injections of large hyperpolarizing current steps into the two cells, we could determine the SPA and coupling co-efficient in each direction¹. Among intra-glomerular pairs we observe there to be extremely non-uniform coupling (ie coupling in one direction can be 5-10 fold greater than in the other¹). As such, no correlation was observed between the

strength of coupling and the difference in sag potential amplitude recorded in the two cells ($r = 0.017$, $n = 26$ pairs). Moreover, the largest coefficient recorded was 0.22 ($n = 125$ pairs; including¹) where the mean is 0.05. Thus hyperpolarizing to -90mV from -50mV in one cell does not produce more than a couple of mV hyperpolarization in the second cell and cannot significantly evoke I_h ($V_{1/2 \text{ max}} = -88 \text{ mV}$;⁴). Importantly, sag was never simultaneously probed in the two cells meaning that electrical coupling cannot contribute directly to the similarity in SPA recorded in intra-glomerular pairs.

Following recordings, DAB staining was performed as previously described¹. Consistent with previous observations^{1,3} all recovered pairs that were observed to be electrically coupled were found to project their apical dendrites to the same glomerulus and never to different glomeruli¹.

Sag analysis

The I_h sag potential was measured as the difference between the peak voltage and the steady-state voltage at the end of the current step (Supplementary Figure 1). The membrane potential difference between the peak and steady-state was abolished by bath application of the specific I_h channel blocker ZD-7288 (Supplementary Figure 1). It is also known that the amplitude of the sag in a given mitral cell is correlated to the amount of I_h current measured in voltage clamp under pharmacological conditions that isolate I_h ⁴ (below). Also, the minimal cell-to-cell variability in, and attenuation of, voltage signals along the apical dendrite^{4,5} does not account for the very substantial (more than an order of magnitude) diversity in somatic sag potential recorded across the mitral cell population⁴. To minimize membrane voltage-related variability in the determination of sag amplitude, only cells with traces falling within

-90 ± 4 mV at steady-state were included in this study. For cells showing negative sag the “peak” voltage was measured at 100 ms after the onset of the hyperpolarizing step.

Voltage clamp recording of I_h

To isolate I_h during whole-cell voltage-clamp recordings we used an external solution without NaH_2PO_4 and CaCl_2 containing (in mM): 105 NaCl, 12.5 KCl, 26 NaHCO_3 , 1 MgCl_2 , 1 CoCl_2 , 10 Tetraethylammonium-Cl (TeaCl), 1 BaCl_2 , 5 4-aminopyridine (4-AP), 0.001 TTX, 0.05 picrotoxin, 0.01 NBQX, 0.05 D-APV. In the presence of the cocktail, electrical coupling between simultaneously recorded mitral cells was again used to determine whether or not cells belonged to the same glomerulus. For simultaneously recorded cells, only pairs with intact apical tufts identified via biocytin fill were analysed. Currents were compensated for series resistance (12 ± 3.5 M Ω , $n = 44$) errors by 50% on-line. No leak subtraction was carried out. I_h amplitude was quantified as the difference between current measured at the onset and the end of the hyperpolarizing voltage step (-50 to -100mV, 2 seconds) excluding capacitive transients. In all cases the digital subtraction of the current recorded in the isolation cocktail before and after application of ZD-7288 (40 μM) was used⁴. The data are expressed as the mean \pm S.E.M.

Data analysis

To determine the extent to which the SPA recorded across the population reflected a uni-modal distribution we used the Dip Test⁶ that returned a dip statistic of 0.0238. To test the significance of this dip statistic we used a bootstrap sample of 50000, resulting in $p = 0.974$, indicating that SPA distribution does not deviate significantly

from unimodality. Unless stated otherwise, all data are reported as the mean \pm the standard deviation. To test the statistical significance between groups we used either paired or non-paired student t-test or, for non-parametric data, the Mann-Whitney U test. Data analysis was performed in Igor Pro, Matlab and Microsoft Excel. For box plots whiskers represent the minimum and maximum values, the bottom and top horizontal lines represent 1st and 3rd quartile respectively, whereas the middle horizontal line represents the median.

For the multiple pair-wise comparison analysis of sag difference, we calculated the modulus of differences in sag potential amplitudes (SPAs) between all recorded cells, i.e. $|\text{SPAcell}_1 - \text{SPAcell}_2|$, $|\text{SPAcell}_1 - \text{SPAcell}_3|$, $|\text{SPAcell}_1 - \text{SPAcell}_4|, \dots, |\text{SPAcell}_1 - \text{SPAcell}_n|$, $|\text{SPAcell}_2 - \text{SPAcell}_3|$, $|\text{SPAcell}_2 - \text{SPAcell}_4|, \dots, |\text{SPAcell}_2 - \text{SPAcell}_n|, \dots, |\text{SPAcell}_{(n-1)} - \text{SPAcell}_n|$, resulting in $(n-1) * (n/2)$ data points when simultaneously recorded pairs are included (Figure 3b1,2, Suppl. Figure 1) or $(n-2) * (n/2)$ data points when simultaneously recorded pairs are excluded (Figure 1e,f). Histograms were generated whereby counts for each bin were expressed as percentage of the total count and fitted using a smoothing spline function (Matlab, Curve Fitting Toolbox) to visualize the disparity of distributions.

Morphological reconstruction

To obtain the morphologies of the cells we recorded from, biocytin (0.4% weight/volume) was included in the patch-pipette solution. Each slice was fixed in 4% PFA immediately after the experiment and stained the day after using the Avidin-Biotin-peroxidase Complex for amplification (ABC kit, Vector Labs) and DAB (1

mg/ml) for visualization⁷. The cells of Figures 1 and 3 were 3D digitally reconstructed by tracing all biocytin-stained arborizations using a NeuroLucida system (Microbrightfield Inc.) under 100x magnification.

Immunohistochemistry

All mice (P28-P35) used for immunohistochemistry were anesthetized using intraperitoneally-administered pentobarbital and subsequently perfusion-fixed in 4% PFA, pH 7.2. The brains were removed and post-fixed in the same fixative overnight. After fixation, the olfactory bulbs were cryoprotected in 30% sucrose-PBS for 5 days, frozen and sectioned horizontally (40 μ m thick).

For HCN2 immunostaining with rabbit polyclonal HCN2, free-floating sections were treated with 1% hydrogen peroxide for 10 min followed by blocking for 30 min in normal donkey serum (code no: 017-000-121, Jackson ImmunoResearch Laboratories, Baltimore, PA, USA) at room temperature. Slices were then incubated with HCN2 rabbit polyclonal antibody (diluted 1:1000; Biomol BML-SA598-0050) overnight at 4°C. Detection of HCN2 was done using a biotinylated rabbit (Fab) 2 (code no: 711-066-152 Jackson ImmunoResearch Laboratories, Baltimore, PA, USA, diluted 1:2000) in combination with the Avidin-Biotin-peroxidase Complex (ABC) (VWR international, Roedovre, Denmark) and followed by 0.05% DAB.

HCN2-DAB images were analyzed for homogeneity across glomeruli using ImageJ (NIH). A region of interest (ROI) was defined manually for each glomerulus. Mean pixel intensities (in arbitrary units) were calculated for all ROIs from all images and pooled into the M71 transgenic (n = 3 mice) or control (n = 3 mice) groups. The two

datasets were tested for equal variance using Levene's test and a one-sided Ansari-Bradley test (for the Ansari-Bradley test each group's median was subtracted from all data points within that group, resulting in equal medians for the two datasets as is required for Ansari-Bradley).

Immunostaining for HCN2 and the OMP-IRES-tau-LacZ: The HCN2 antibody (1:5000) was visualized as described above (secondary antibody diluted 1:800) and the signal was enhanced with biotinylated tyramide (Tyramide System Amplification, PerkinElmer Waltham, MA, USA) and visualized by streptavidin-488 (code no: 016-488-084 Jackson ImmunoResearch Laboratories, Baltimore, PA, USA, diluted 1:500). This reaction was followed by incubation with a mouse anti- β -galactosidase (Sigma-Aldrich B0271, diluted 1:5000) visualized using a donkey anti-mouse conjugated Alexa-594 (code no: A-21203, Molecular Probes, USA, diluted 1:800).

Analysis for co-localization of HCN2 and β -gal-positive axons was performed as described previously⁸ using high-resolution confocal microscopy (Olympus IX70 or Zeiss LSM 510) to generate stacks of 40-90 images (0.23-0.30 μ m) equal to a scan depth of 9.2-20.7 μ m (Z-axis). Intensity of the channels was carefully adjusted within the borders of the grey tone scale to preserve information about relative intensities in the digital image and to prevent overexposure. Volocity 3.6 (Improvision, Coventry, UK) was used for the analysis that consisted of de-convolution of each stack of images (using the Restoration module and fast restoration based on a calculated Point Spread Function) followed by co-localization analysis of 3D rendered images. Cellular extension was determined by the Classification module of Volocity following a set of well-defined criteria in which the lower threshold level of fluorescent

intensity defining cellular borders was set as high as possible under consideration of maintaining a natural three-dimensional image of the cyto-architecture (Figure 2b-d). To eliminate user bias, the threshold was set independently for each of the three channels. Given these conditions, co-localization (overlap) was calculated (using the Classification module) and visualized using the 3D-rendering function (using the Visualization module). Image-editing software (Adobe Photoshop and Adobe Illustrator; Adobe Systems, San Jose, CA) was used to combine the obtained images into plates.

References

- 1 Pimentel, D. O. & Margrie, T. W. Glutamatergic transmission and plasticity between olfactory bulb mitral cells. *J Physiol* **586**, 2107-2119 (2008).
- 2 Schoppa, N. E. & Westbrook, G. L. AMPA autoreceptors drive correlated spiking in olfactory bulb glomeruli. *Nat Neurosci* **5**, 1194-1202 (2002).
- 3 Christie, J. M. *et al.* Connexin36 mediates spike synchrony in olfactory bulb glomeruli. *Neuron* **46**, 761-772 (2005).
- 4 Angelo, K. & Margrie, T. W. Population diversity and function of hyperpolarization-activated current in olfactory bulb mitral cells. *Scientific Reports* **1**, doi:10.1038/srep00050 (2011).
- 5 Djuricic, M., Antic, S., Chen, W. R. & Zecevic, D. Voltage imaging from dendrites of mitral cells: EPSP attenuation and spike trigger zones. *J Neurosci* **24**, 6703-6714 (2004).
- 6 Hartigan, J. A. & Hartigan, P. M. The Dip Test of Unimodality. *Annals of Statistics* **13**, 70-84 (1985).
- 7 Horikawa, K. & Armstrong, W. E. A versatile means of intracellular labeling: injection of biocytin and its detection with avidin conjugates. *Journal of Neuroscience Methods* **25**, 1-11 (1988).
- 8 Ostergaard, J., Hannibal, J. & Fahrenkrug, J. Synaptic contact between melanopsin-containing retinal ganglion cells and rod bipolar cells. *Invest Ophthalmol Vis Sci* **48**, 3812-3820, (2007).